Nonlinear patterns in Bose-Einstein condensates in dissipative optical lattices

Yu. V. Bludov[1,*] and V. V. Konotop[2,†]

[1]*Centro de Física, Universidade do Minho, Campus de Gualtar, Braga P-4710-057, Portugal*

[2]*Centro de Física Teórica e Computacional, Universidade de Lisboa, Complexo Interdisciplinar, Avenida Professor Gama Pinto 2, Lisboa P-1649-003, Portugal, and Departamento de Física, Universidade de Lisboa, Campo Grande, Ed. C8, Piso 6, Lisboa P-1749-016, Portugal*

(Received 6 August 2009; revised manuscript received 11 November 2009; published 26 January 2010)

It is shown that the one-dimensional nonlinear Schrödinger equation with a dissipative periodic potential, nonlinear losses, and a linear pump allow for the existence of stable nonlinear Bloch states which are attractors. The model describes a Bose-Einstein condensate with inelastic two- and three-body interactions loaded in an optical lattice with losses due to inelastic interactions of the atoms with photons.

DOI: 10.1103/PhysRevA.81.013625 PACS number(s): 03.75.Kk, 03.75.Lm, 67.85.Hj

I. INTRODUCTION

Being an indispensable attribute of all natural processes, the dissipation accompanied by properly adjusted compensation of losses plays a constructive role in the generation of nonlinear patterns that are observed in many natural sciences, including physics, biology, chemistry, and life sciences [1]. As attractors, the respective structures play a prominent role in practical applications, among which we particularly mention light patterns in nonlinear optics, which are receiving a rapidly increasing amount of attention [2]. Several mathematical models have been developed for the description of the emergence of dissipative patterns, the complex Ginzburg-Landau equation being the most simple and widely used one. This model allows for quantitative and often even qualitative descriptions of a wide range of physical phenomena [3].

The dissipation is also an important factor in the theory of Bose-Einstein condensates (BECs), where it appears in a natural way either through the inelastic interactions of light with atoms (see, e.g., [4]) or in a form of inelastic two-body and three-body interatomic interactions [5–7]. Alternatively, the dissipation can be introduced artificially, say, in the form of a nonlinear dissipative lattice [8] or by probing the condensate by means of an electronic beam [9], and can affect the matter wave dynamics in a variety of ways [10]. It is then natural to expect that a BEC where the dissipative losses are properly compensated by an atom pump into the system, can give rise to highly stable atomic density distributions. Probably the simplest nontrivial and practically important realization of such a situation can be a BEC loaded into a one-dimensional (1D) optical lattice (OL).

This leads us to the aim of the present work: We report on a theoretical study of stable matter wave patterns emerging in an array of BECs when the linear and nonlinear dissipations are compensated by a homogeneous atom pump. More specifically, we show that in such systems, the emergence of *nonlinear dissipative Bloch waves* is possible. Such periodic patterns appear as attractors, and hence initial distributions in a large range of the parameters rapidly evolve into the dissipative Bloch waves. These are essentially nonlinear states, which in a general situation do not allow for transition to the limit of zero density, and at the same time, when the dissipation is not too strong, can be naturally associated with a specific edge of the band of the underlying conservative part of the lattice potential.

The organization of the present article is as follows. In Sec. II we formulate the models of the dissipative cubic nonlinear Schrödinger (NLS) equation and provide estimates for the main effects to be observable. In Sec. III we perform numerical study of the emergence and stability of the periodic patterns. Section IV is devoted to extending the results to the NLS equation with quintic dissipation. In Sec. V we present the respective lattice models, which can be obtained using the tight-binding approximation from the initial continuous dissipative NLS equations. The results are summarized in the Conclusion, Sec. VI.

II. THE MODEL AND ANALYTICAL ESTIMATES

A. The model

We start with the 1D Gross-Pitaevskii (GP) equation,

$$i\Psi_t = -\Psi_{xx} + 2\alpha \sin^2(x)\Psi + g|\Psi|^2\Psi + i\Gamma\Psi, \qquad (1)$$

where $\alpha = \alpha' - i\alpha''$ is the properly normalized complex atomic polarizability whose imaginary part $\alpha'' > 0$ becomes appreciable for relatively large electric fields (see, e.g., [4]), $g = g' - ig''$ is the dissipative nonlinearity (with $g'' > 0$ describing inelastic interatomic collisions), and $\Gamma > 0$ is the linear gain.

It is relevant to mention that emergence of coherent localized and periodic structures from the interplay between periodicity and complex (i.e., conservative and dissipative) nonlinearity has recently being addressed within the framework of the complex Ginzburg-Landau equation [11], and nonlinear dissipative Bloch waves in a model of optical parametric oscillators were reported in Ref. [12]. Compared to these previous studies, apart from the physical applications, the present model (1) displays very different mathematical features, which stem from the periodically varying dissipation which is controlled by the OL.

For the next consideration it is convenient to introduce the parameter

$$\Delta = \Gamma - \alpha'', \qquad (2)$$

*bludov@fisica.uminho.pt
†konotop@cii.fc.ul.pt

which will play the role of the effective gain (discussed later in this article), and the parameter ϕ, defined by the relations $g''/|g| = \sin\phi$ and $g'/|g| = \cos\phi$, which controls the nonlinear dissipation (the parametrization introduced implies that $0 \leqslant \phi \leqslant \pi$). Then, renormalizing the macroscopic wave function $\psi = |g|^{1/2} e^{-i\alpha' t}\Psi$, we rewrite Eq. (1) in the form

$$i\psi_t = -\psi_{xx} - (\alpha' - i\alpha'')\cos(2x)\psi + e^{-i\phi}|\psi|^2\psi + i\Delta\psi. \tag{3}$$

B. On a homogeneous linear pump

The model (3) explored in the present article is based on the supposition that there exists some "gain" mechanism compensating for dissipative losses. Generally speaking, such a mechanism would require an infinite external reservoir of atoms supplying the condensate. Inclusion of the linear gain has been explored in the BEC applications [5,13] and is usually associated with the growth of the number of condensed atoms due to condensation from the thermal cloud [5].

In this subsection we outline an idea on how an *effective* homogeneous gain can be implemented "mechanically." It is based on the fact that what really matters is the linear atomic density rather than the total number of atoms. Hence, one can consider a cigar-shaped condensate whose dimensions decrease in time, thus resulting in increasing linear density.

To this end, we consider a 1D BEC loaded into a cigar-shaped potential, which consists of a periodic OL and a parabolic trap. In order to implement an effective linear homogeneous pump, we assume that (i) both the longitudinal and the transverse harmonic oscillator frequencies are growing functions of time: $\omega_\parallel(T) = \omega_\parallel f(T)$ and $\omega_\perp(T) = \omega_\perp f(T)$, where $\omega_\parallel$ and $\omega_\perp$ are the respective frequencies at initial time $T = 0$ and $f(T)$ is a positive definite increasing function, chosen to be $f(T) \equiv (1 - 2\omega_\parallel T)^{-1}$; (ii) the complex s-wave scattering length grows over time: $a(T) = a_s f(T)$, $a_s = a_s' - i a_s''$ being the initial complex scattering length (the desired time dependence can be achieved with the help of the Feshbach resonance); (iii) the lattice amplitude and the lattice period are functions of time: $V(T) = Vf(T)$ and $d(T) = df^{-1/2}(T)$, $V = V' - iV''$ and d being the respective initial values (this can be achieved by changing the laser-beam intensity and the angle between the beams creating the OL). Then, in the mean-field approximation such a condensate is described by the 3D GP equation with varying coefficients,

$$\begin{aligned} i\hbar\Psi_T = &-\frac{\hbar^2}{2m}\nabla^2\Psi + 2V(T)\sin^2\left[\frac{\pi X}{d(T)}\right]\Psi \\ &+ \frac{m}{2}[\omega_\parallel^2(T)X^2 + \omega_\perp^2(T)R_\perp^2]\Psi + \frac{4\pi\hbar^2 a(T)}{m}|\Psi|^2\Psi, \end{aligned} \tag{4}$$

where Ψ and m are the wave function (in the physical units) and the mass of the atoms, respectively, and $\mathbf{R}_\perp = (Y, Z)$ is the transverse coordinate.

In the case when the OL period d is much bigger than the transverse harmonic oscillator length, $d \gg a_\perp = \sqrt{\hbar/(m\omega_\perp)}$, Eq. (4) can be reduced to the 1D GP equation by means of the multiple-scale expansion procedure [14]. To this end, the 3D bosonic wave function has to be searched in the form

$$\begin{aligned} &\Psi(X, \mathbf{R}_\perp, T) \\ &= \frac{\pi a_\perp}{2d|a_s|^{1/2}}\psi(x,t)\zeta(\mathbf{R}_\perp, T) \\ &\times \exp\left\{-i\frac{V'T}{\hbar} - i\frac{\omega_\perp}{2\omega_\parallel}\ln[f(T)] - i\frac{\omega_\parallel f(T)X^2}{2\omega_\perp a_\perp^2}\right\}, \end{aligned} \tag{5}$$

where $\psi(x,t)$ is the unknown dimensionless function of the new dimensionless independent variables

$$x = \frac{\pi}{d}\sqrt{f(T)}X \quad \text{and} \quad t = \frac{E_r}{2\hbar\omega_\parallel}\ln[f(T)] \tag{6}$$

(hereafter $E_r = \hbar^2\pi^2/(2md^2)$ is the "initial" recoil energy), and $\zeta(\mathbf{R}_\perp, T) = \pi^{-1/2}a_\perp^{-1}\exp[-R_\perp^2 f(T)/(2a_\perp^2)]$ describes the linear transverse distribution varying in time due to the change of the transverse trap. Then, introducing the dimensionless parameters $\alpha = \alpha' - i\alpha'' = (V' - iV'')/E_r$, $\Delta = 3\hbar\omega_\parallel/(2E_r) - \alpha''$, and ϕ, the latter defined by the relations $a_s''/|a_s| = \sin\phi$ and $a_s'/|a_s| = \cos\phi$, and substituting the ansatz (5) in Eq. (4), one readily obtains the desirable Eq. (3).

It is clear that the aforementioned mechanism formally works only for $T < 1/2\omega_\parallel$ and implies change of the trap dimensions, which should not affect the applicability of the mean-field model.[1] This means that the created effective pump is relatively small and thus can properly work for small dissipative losses. For example, if in the dimensionless units $\Gamma \sim \alpha'' \sim 0.001$, for the rubidium condensate loaded in a cigar-shaped trap with the initial dimensions $a_\perp = 0.5\ \mu$m and $a_\parallel = 17.32\ \mu$m (corresponding to the $\omega_\parallel \approx 2.42$Hz) and with the imposed OL with the constant $d = 1\ \mu$m, one computes that the time interval during which the constant pump can be supported is $T \approx 155$ ms (or $t \approx 1040$ in dimensionless units) and corresponds to the decrease of the linear dimensions of the trap two times.

In this work, however, we explore more strong values of the gain (and dissipation) in order to reduce the time during which instabilities are developed and unstable initial conditions converge to the respective attractors. More specifically, following [6] for all numerical simulation we will choose $\Gamma = 0.1$.

C. On the spectrum of the linear problem

We are particularly interested in periodic stationary patterns. Therefore, we explore the ansatz $\psi(x,t) = \varphi(x)\exp(-i\mu t)$, with a real chemical potential μ leading the nonlinear eigenvalue problem

$$\mu\varphi = L\varphi + i[\Delta + \alpha''\cos(2x)]\varphi + e^{-i\phi}|\varphi|^2\varphi, \tag{7}$$

where we have introduced the linear operator $L = -\frac{d^2}{dx^2} - \alpha'\cos(2x)$. The eigenvalues and eigenfunctions of this operator

[1]The consideration in this article was restricted to 1D models, whose validity is well justified in the limit of low densities and tight transverse binding (see, e.g., [14]). The full 3D simulations accounting for possible transverse effects will be published elsewhere.

are obtained from the Mathieu equation

$$L\varphi_{nk} = E_n(k)\varphi_{nk}. \tag{8}$$

It gives the band-gap spectrum, characterized by the number of the band $n \geqslant 1$ ($n = 1$ corresponding to the lowest band) and by the wave vector k in the first Brillouin zone, $k \in [-1, 1]$. Subsequently, the spectrum of the operator L is given by $E_n(k) \in [E_1^{(-)}, E_1^{(+)}] \cup [E_2^{(-)}, E_2^{(+)}] \cup \cdots (E_1^{(-)} < E_1^{(+)} < E_2^{(-)} < \ldots)$. Here $E_n^{(-)}$ and $E_n^{(+)}$ are, respectively, the lower and the upper edges of the nth band; $E_n^{(-)} = E_n(0)$, $E_n^{(+)} = E_n(1)$ if n is odd, and $E_n^{(-)} = E_n(1)$, $E_n^{(+)} = E_n(0)$ if n is even.

The requirement for μ to be real readily gives the relation

$$\int_0^\pi [\alpha'' \cos(2x)|\varphi|^2 - \sin(\phi)|\varphi|^4]dx + \Delta N = 0, \tag{9}$$

where $N = \int_0^\pi |\psi|^2 dx$ is the normalized number of atoms per one lattice period. We notice that the condition (9) can also be obtained from the requirement for the number of condensed atoms to conserve, that is, from $\partial N/\partial t \equiv 0$.

Our analysis will be restricted to the case of weak dissipation, which we express in terms of the small parameter $\varepsilon = \sqrt{|\alpha''/\alpha'|} \ll 1$ and, respectively, we require $\Delta = \varepsilon^2\delta$ with $|\delta| \lesssim 1$. It is then natural to recall that, in the absence of the dissipation, Eq. (3) possesses branches of periodic solutions which in the linear limit, that is, when $N \to 0$, are reduced to the conventional Bloch states φ_{nk}. Moreover, when $N \ll 1$, the modulational instability of the respective periodic solutions is described in terms of the multiple-scale approximation [14]. Therefore, we start the description of the dissipative problem at hand with this limit.

As the first step, we consider the case when in the respective linear problem

$$L\varphi + i\varepsilon^2 V(x)\varphi = E\varphi, \tag{10}$$

the dissipation $V(x) \equiv \delta + \alpha' \cos(2x)$ is treated as a perturbation. Straightforward application of the perturbation theory allows to obtain corrections for a chosen eigenvalue $E_n(k)$ due to the dissipative term

$$E = E_n(k) + \varepsilon^2 E_{nk}^{(1)} + \varepsilon^4 E_{nk}^{(2)} + \cdots, \tag{11}$$

with

$$E_{nk}^{(1)} = i\int_0^\pi V(x)|\varphi_{nk}(x)|^2 dx \tag{12}$$

and

$$E_{nk}^{(2)} = -\sum_{n' \neq n} \frac{\left|\int_0^\pi V(x)\varphi_{nk}(x)\overline{\varphi}_{n'k}(x)dx\right|^2}{E_n(k) - E_{n'}(k)} \tag{13}$$

(hereafter an overbar stands for the complex conjugation). The obtained result has several important consequences. Indeed, for the eigenvalue to be real, one has to require $E_{nk}^{(1)} = 0$, or explicitly,

$$\Delta + \alpha''\gamma = 0, \quad \gamma = \int_0^\pi \cos(2x)|\varphi_{nk}(x)|^2 dx. \tag{14}$$

This requirement for the eigenvalues to be real either cannot be satisfied or can be satisfied only for a single gap edge [since γ depends on the indexes (n, k) which are omitted for the sake of brevity of notations]. Thus, in a general situation $\Delta \neq 0$. If $\Delta < -\alpha''\gamma$, then $E_{nk}^{(1)}$ describes effective dissipation, which means that the zero solution ($\psi \equiv 0$) is an attractor. If, however, $\Delta > -\alpha''\gamma$, the zero solution becomes unstable and one should expect the emergence of nonlinear coherent structures, which of course are possible if the respective linear pump is compensated by the nonlinear dissipation. This is precisely the case of $\sin\phi > 0$ in the parametrization chosen earlier in this article [see also Eq. (9)].

For $\Delta = 0$ (this is the situation explored in all numerical simulations reported in this article), the aforementioned arguments mean that the nonlinear stable structures are expectable only for $\gamma > 0$. Then nonlinear patterns are generated from arbitrarily small initial fluctuations (see also Fig. 2). In the meantime, the sign of γ is not uniquely defined and depends on the band-gap edge. For the cos-like lattice, explored here, positive γ is verified only for the lowest bands. Hence, only close to the lowest band edges can one expect to obtain low-density stable nonlinear patterns. This conjecture is verified for all numerical simulations performed in the present article.

Finally, we observe the validity of the inequality

$$|\gamma| < 1, \tag{15}$$

which will be used for the discussion in what follows.

D. Multiple-scale analysis of the stability

By varying the pump one can *selectively excite periodic patterns*, whenever more than one stable state exists. In the low-density limit (i.e., at $N \to 0$), the stability of the periodic solutions can be tested using the multiple-scale analysis, similar to the approach successfully used in the conservative case [14]. Now ε has to be used as a small parameter of the problem. Following this approach, for the chosen band edge, say $E_n^{(\pm)}$, the wave function is approximated by $\psi \approx \varepsilon A(\xi, \tau)\varphi_n^{(\pm)}(x)\exp[-iE_n^{(\pm)}t]$, where $A(\xi, \tau)$ is an amplitude depending on slow variables $\xi = \varepsilon x$ and $\tau = \varepsilon^2 t$ and $\varphi_n^{(\pm)}(x)$ is the Bloch wave function at the edge of the nth band. We observe that by choosing ε to be the small parameter we implicitly impose the conditions where the characteristic scale of the excitations is determined by the complex part of the potential (contrary to case of a conservative system, where the small parameter of expansion is treated as a free parameter related to the detuning of the chemical potential toward the adjacent gap; see, e.g., [14]).

Using the standard algebra (the details can be found in Ref. [14]), one verifies that $A(\xi, \tau)$ solves the dissipative NLS equation

$$iA_\tau = -(2M)^{-1}A_{\xi\xi} + i\Lambda A + e^{-i\phi}\chi|A|^2 A. \tag{16}$$

Here $M = (d^2E_n^{(\pm)}/dk^2)^{-1}$ is the effective mass,

$$\Lambda = \alpha'\gamma + \delta = \frac{\alpha''\gamma + \Delta}{\varepsilon^2} \tag{17}$$

is the effective gain (according to the analysis of Sec. II C, nonlinear patterns emerge near edges with $\Lambda > 0$, a conclusion that is also confirmed by the following analytical consideration and numerical simulations, which justify the definition of Λ as a gain),

$$\chi = \int_0^\pi |\varphi_n^{(\pm)}|^4 dx \tag{18}$$

is the effective nonlinearity, and γ is defined in (14) with $\varphi_{nk} = \varphi_n^{(\pm)}$. Within the framework of the multiple-scale expansion, the condition (9) for conservation of the number of atoms can be recast as follows:

$$\Lambda - \sin(\phi)\chi|A|^2 = 0. \tag{19}$$

Equation (16) possesses a stationary, coordinate-independent solution in the form

$$A_{st} = \sqrt{\frac{\Lambda}{\chi \sin(\phi)}} e^{-i\Omega\tau}. \tag{20}$$

Here $\Omega = \Lambda/\tan(\phi)$ is a constant determining the shift of the chemical potential outward from the gap edge: recall that now $\mu = E_n^{(\pm)} + \varepsilon^2\Omega$. Unlike in the case of conservative systems, the value of Ω is fixed. It is determined by the linear density of atoms and by the nonlinear dissipation controlled by the parameter ϕ through the relations

$$N = \frac{\alpha''\gamma + \Delta}{\chi \sin\phi}, \qquad \mu = E_n^{(\pm)} + \frac{\alpha''\gamma + \Delta}{\tan(\phi)}. \tag{21}$$

Several important conclusions follow immediately from Eqs. (21). First, the limit $N \to 0$ can be reached only when the condition (14) is satisfied, that is, only subject to the requirement for the spectrum to be real. In this limit, $\mu \to E_n^{(\pm)}$. For the general case, one must have $N > 0$, which leads us to the condition on the linear dissipation $\alpha''\gamma + \Delta > 0$ necessary for existence of the nonlinear periodic solutions. This constraint, which in Sec. II C was obtained form the analysis of the linear spectrum, is equivalent to the requirement $\Lambda > 0$ in Eq. (16), and under the chosen parametrization of nonlinearity, phase ϕ is necessary for the particle conservation (19). In the original notations, the obtained necessary condition reads $\Gamma > (1-\gamma)\alpha''$ and means that the pump should be stronger than the dissipation α'' reduced by the lattice factor $(1-\gamma)$ [notice that due to (15), this is a positive factor]. Now the number of particles per one OL period cannot be smaller than the minimal value $N_{\min} = (\alpha''\gamma + \Delta)/\chi$, which is the number of particles in the case of pure dissipative nonlinearity [i.e., when $(\phi = \pi/2)$]. In this limit, $\mu \to E_n^{(\pm)}$.

As the second relevant property of the system at hand, following from (21) we emphasize that the chemical potential is not a free parameter, as would happen in a conservative system, but is determined by the balance of incoming and dissipating atoms. This balance can be controlled, say, by the nonlinear dissipation, parametrized by ϕ. Respectively, obtaining solutions corresponding to different branches [see, e.g., Figs. 1(b) and 1(d)] requires changing the nonlinear dissipation. In practical terms this can achieved, say, by using variations of the light with a frequency close to resonance with one of the excited atomic states. Then the control parameter between the real and the imaginary parts of the scattering length is the relation between the frequency detuning $\tilde{\delta}$ form the excited level and the natural line width $\tilde{\Gamma}$, $\tilde{\delta}/\tilde{\Gamma}$ [6], and practically any value of the parameter ϕ is achievable (see, e.g., the examples considered in [6]).

As is customary, to check the stability of constant-amplitude solutions, we consider small perturbations of the stationary solution: $A_{\rm st} + (ae^{ik\xi - i\omega\tau} + \bar{b}e^{-ik\xi + i\bar{\omega}\tau})e^{-i\Omega\tau}$ (here $|a|, |b| \ll |A_{\rm st}|$). Substituting this ansatz in Eq. (16) and linearizing with respect to a and b, we obtain a dispersion relation in the long-wavelength limit ($k \ll 1$):

$$\omega = -i\Lambda \pm \sqrt{\Omega k^2/M - \Lambda^2}. \tag{22}$$

Thus, for the stability of the background A, we have to require two conditions:

$$\Lambda > 0 \quad \text{and} \quad [\mu - E_n^{(\pm)}]M > 0. \tag{23}$$

The first of these inequalities has the simple meaning of positive effective dissipation, which must compensate for the nonlinear losses. The second condition is of "conservative origin" and coincides with the stability of Bloch states in the conservative systems (see, e.g., [14]).

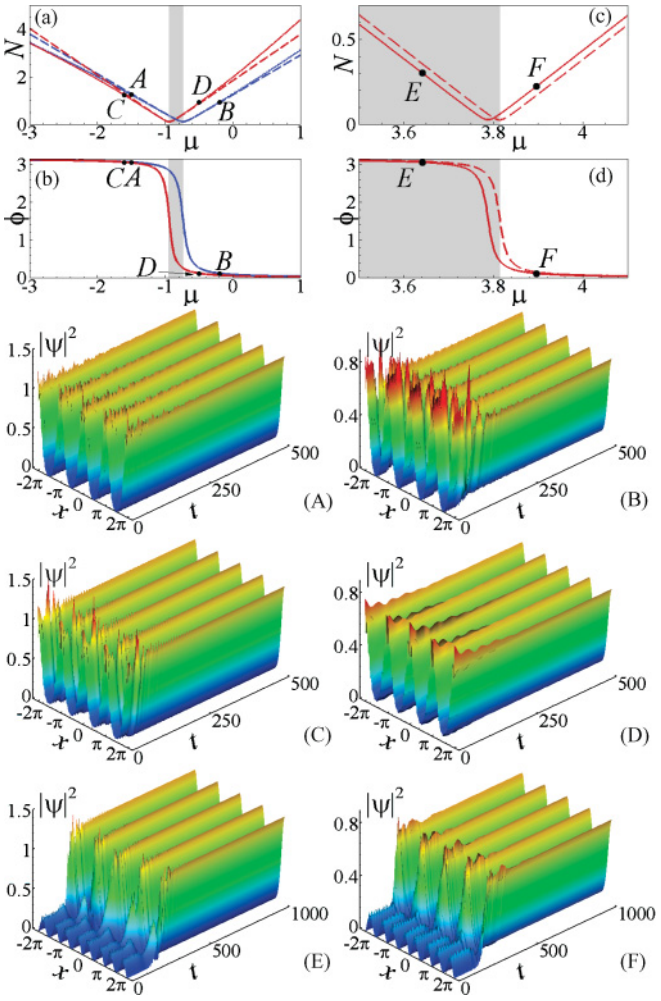

FIG. 1. (Color online) The number of particles N [panels (a) and (c)] and the phase of the nonlinearity, ϕ [panels (b) and (d)] vs the chemical potential μ for $\alpha' = 3.0$, $\alpha'' = 0.1$, and $\Delta = 0.0$ obtained analytically (dashed lines) from Eqs. (21) and numerically (solid lines). Gray strips represent the first [in panels (a) and (b)] and the second [in panels (c) and (d)] bands. Panels (A)–(F) illustrate temporal evolution of periodic solutions corresponding to the respectively labeled points in panels (a)–(d). Points A, C, and E are chosen to have the same nonlinearity phase $\phi \approx 3.055$. Similarly, points B, D, and F are characterized by the phase $\phi \approx 0.116$. The corresponding parameters γ are $\gamma = 0.641$ [panels (A) and (B)], $\gamma = 0.536$ [panels (C) and (D)], and $\gamma = 0.123$ [panels (E) and (F)].

Besides the stationary solution (20), Eq. (16) possesses a time-dependent homogeneous solution,

$$A(\tau) = a(\tau)\exp\left[-i\cos(\phi)\chi\int_{\tau_0}^{\tau} a^2(\tau')d\tau'\right], \tag{24}$$

where

$$a(\tau) = \frac{\sqrt{\Lambda}a_0}{\sqrt{\Lambda e^{2\Lambda(\tau_0-\tau)} + \chi\sin(\phi)a_0^2[1-e^{2\Lambda(\tau_0-\tau)}]}},$$

$a_0 = a(\tau_0)$, and τ_0 is the initial time.

For a positive Λ and nonzero a_0, the distribution (24) at $\tau \to \infty$ converges to the stationary solution (20). In other words, the pattern (20) is an attractor for any nontrivial initial distributions, corresponding to a smoothly modulated Bloch function. The respective time dependence of the particle number per period can be represented as

$$N = \frac{N_0(\alpha''\gamma + \Delta)}{N_0\chi\sin\phi + e^{2(\alpha''\gamma+\Delta)(t_0-t)}(\alpha''\gamma + \Delta - N_0\chi\sin\phi)}, \tag{25}$$

where N_0 is the initial number of particles and we restored to the original dimensionless variables.

Later in this article we will also explore the dynamical regimes where after some interval of time the pump is switched off, that is, $\Gamma = 0$ and $\Delta = -\alpha''$ (respectively, $\delta = -\alpha'$). Recalling the definition (17) as well as the property (15), we conclude that this is the case of $\Lambda = \alpha'(\gamma - 1) < 0$. Now the particle conservation condition (19) cannot be met for the dissipative nonlinearity $\sin(\phi) > 0$. It is evident that in this case, nonstationary solution (24) evolves toward zero; that is, the zero solution becomes an attractor. The respective dependence of the number of particles per period on time is now expressed as

$$N(t) = \frac{N_0\alpha''(1-\gamma)e^{2\alpha''(\gamma-1)(t-t_0)}}{\alpha''(1-\gamma) + N_0\chi\sin(\phi)[1-e^{2\alpha''(\gamma-1)(t-t_0)}]}. \tag{26}$$

At $t - t_0 \gg [\alpha'']^{-1}$, this decay has the exponential asymptotic

$$N(t) \approx \frac{N_0\alpha''(1-\gamma)}{\alpha''(1-\gamma) + \chi\sin(\phi)N_0}e^{2\alpha''(\gamma-1)(t-t_0)}. \tag{27}$$

III. NUMERICAL STUDY OF COHERENT STRUCTURES

When the external parameters of the system (i.e., α', α'', Δ, and ϕ) are fixed, with each band edge one can associate only one solution, having the number of particles and the chemical potential determined from (21) and varying when either of the parameters is changed. Bearing in mind physical applications of the model, we concentrate on the study of the dependence of the number of particles on the chemical potential $N(\mu)$ [which is the same as $N(\Omega)$ due to the link between Ω and μ]. The respective analysis was performed for the lowest bands and is summarized in Fig. 1.

The first lowest band ($n = 1$) is associated to two branches of periodic solutions of Eq. (3) depicted in Figs. 1(a) and 1(b). One branch is 2π periodic (the branch A–B), having zeros of the density in maxima of the OL in Eq. (1); that is, $x_p = \pi/2 + p\pi$ (where p is an integer). For this branch, the dependence $N(\mu)$ reaches its minimum in the vicinity of $E_1^{(+)}$. The second branch is π periodic (branch C–D). It has no zeros in the whole space, reflecting the fact that the respective linear Bloch wave of the underlying conservative system has no zeros. The dependence $N(\mu)$ of the second branch reaches minimum at $E_1^{(-)}$. We notice that analytical expressions for $N(\mu)$ and $\phi(\mu)$ in the vicinity of $E_1^{(\pm)}$ match remarkably well the numerical ones [respectively, dashed and solid lines in Figs. 1(a) and 1(b)].

Turning to the upper edges, in Figs. 1(c) and 1(d) we show the branch E–F, which is associated with the upper edge of the second band. It has the minimum of the number of particles in the vicinity of $E_2^{(+)}$ given by $N_{\min} \approx 0.026$, that is, smaller than the one in the vicinity of first band edges [$N_{\min} \approx 0.1$, see Fig. 1(a)]. We also clearly observe that the minimum of $N(\mu)$ is considerably shifted to the lower values of μ in comparison with the analytical prediction (21).

Passing to the stability of the solutions, direct numerical integration of Eq. (3) reveals that 2π-periodic patterns are stable at $\mu < E_1^{(+)}$ [solution A in Figs. 1(a) and 1(b) and correspondent dynamics in Fig. 1(A)] and unstable at $\mu > E_1^{(+)}$ [solution B in Figs. 1(a) and 1(b) and correspondent dynamics in Fig. 1(B)]. As this is typical for dissipative systems, the stable solution is an attractor, and therefore an unstable initial condition rapidly evolves toward the stable one having the same nonlinear phase ϕ. This process is illustrated in Fig. 1(B), where the unstable solution transforms into the attractor corresponding to the point D [cf. Figs. 1(B) and 1(D)]. At the same time π-periodic solutions are stable at $\mu > E_1^{(-)}$ [see, e.g., solution D in Figs. 1(a) and 1(b) and correspondent dynamics in Fig. 1(D)] and unstable at $\mu < E_1^{(-)}$ [see, e.g., solution C in Figs. 1(a) and 1(b) and correspondent dynamics in Fig. 1(C)], where we show the convergence of the unstable solution to the attractor corresponding to the point A.

The described stability properties corroborate well with the simple analysis performed in the preceding sections. This is not the case, however, for the solutions associated with the upper band edges. They appear to be dynamically unstable, again rapidly converging to the stable lower branches having the same parameter ϕ. This is illustrated by the evolution of the patterns corresponding to points E and F shown in the respective panels of Fig. 1, where they transform into the solutions corresponding to points A and D, respectively. This, however, should not be viewed as the discrepancy with the preceding analysis of the stability. Indeed, the latter one is done for slowly varying perturbations, thus representing only a necessary but not yet sufficient condition for the stability. Moreover, the reported behavior well agrees with the conclusion about emergence of complex eigenvalues due to weak dissipation [see (14), as well as the subsequent discussion].

Having discussed the stability properties of the periodical patterns, we address the following two natural questions: How one can generate the aforementioned stable periodical patterns? And how do they evolve if after some time the gain is off? The answer to the first question is rather simple. Since the final pattern is an attractor, it will be generated from any initial distribution having small density. This is illustrated in Figs. 2(a) and 2(b), where one observes evolution of a homogeneous nonzero excitation toward the *stable* periodic

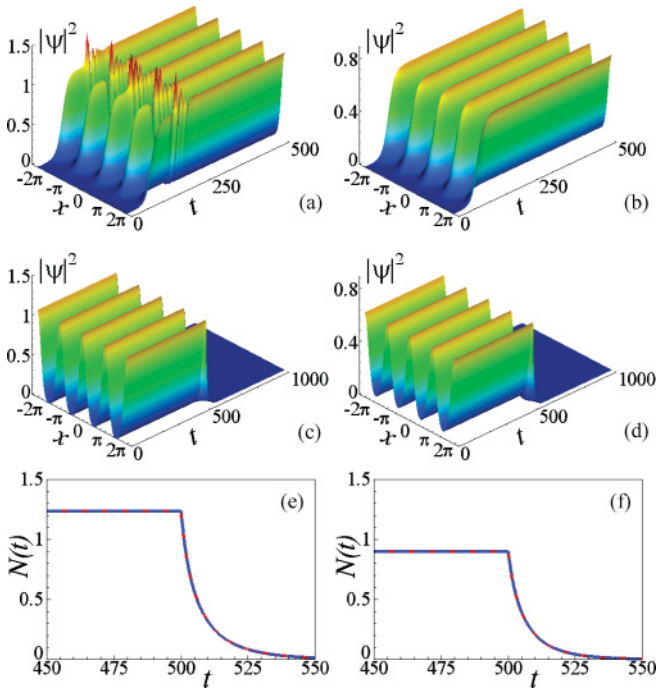

FIG. 2. (Color online) (a), (b) The evolution of the density, obtained from the numerical integration of Eq. (3) with the initial condition $\psi(x,0) \equiv 0.01$. (c), (d) The evolution of the density started with the stable patterns corresponding to points A and D of Fig. 1 with the gain turned off at $t_0 = 500$. (e), (f) Evolution of the number of particles per one period corresponding to the dynamics shown in panels (c) and (d), respectively, calculated numerically (solid curves) and analytically from Eq. (26) (dashed curves). Notice that the solid and dashed curves are indistinguishable on the scale of panels (e) and (f). The other parameters are $\alpha' = 3.0$, $\alpha'' = 0.1$, $\Delta = 0.0$, and $\phi \approx 3.055$ [panels (a), (c), (e)] and $\phi \approx 0.116$ [panels (b), (d), (f)].

pattern, whose parameters (number of particles per OL period and chemical potential) are determined by the fixed phase ϕ of the nonlinearity. More specifically, in Fig. 2(a) the initial excitation is transformed into the solution corresponding to point A in Fig. 1, while the initial excitation in Fig. 2(b) evolves toward the solution with the parameters of the point D in Fig. 1. It is worth noticing that such a spatiotemporal evolution confirms the behavior, qualitatively predicted by Eq. (24).

The answer to the second of the aforementioned questions becomes evident from Figs. 2(c)–2(f), where we show the evolution of the stable periodic patterns after the gain is turned off (recall that turning off the gain is equivalent to setting $\Delta = -\alpha''$). Thus, after turning off the gain, the condensate starts losing the atoms and its density homogeneously goes to zero [as was predicted by Eq. (26)]. Figures 2(e) and 2(f) demonstrate remarkably good correspondence between the numerical results and the analytical predictions.

IV. COHERENT STRUCTURES WITH QUINTIC DISSIPATION

Significant dissipative losses in a BEC can occur due to the inelastic three-body interactions [5–7]. Therefore, as the next step we address their effect on the emergence of the coherent structures in the dissipative model

$$i\Psi_t = -\Psi_{xx} + 2\alpha \sin^2(x)\Psi + g'|\Psi|^2\Psi + i\Gamma\Psi - ig''|\Psi|^4\Psi, \tag{28}$$

where $g'' > 0$, and other parameters are defined as described earlier in this article. Similar to the previous case, introducing the parameters $\Delta = \Gamma - \alpha''$, $g = g'/\sqrt{g''}$, and the renormalized macroscopic wave function $\psi = (g'')^{1/4} e^{-i\alpha' t}\Psi$, we arrive at the equation

$$i\psi_t = -\psi_{xx} - (\alpha' - i\alpha'')\cos(2x)\psi + i\Delta\psi + g|\psi|^2\psi - i|\psi|^4\psi. \tag{29}$$

Now the conservation of the number of atoms requires [cf. Eq. (9)]

$$\int_0^\pi [\alpha'' \cos(2x)|\psi|^2 - |\psi|^6]dx + \Delta N = 0. \tag{30}$$

Following the approach developed earlier in this article for the analysis of the cubic dissipative term, now we employ the multiple-scale analysis of Eq. (29) representing the wave function in the form $\psi \approx \varepsilon^{1/2} A(\xi,\tau)\varphi^{\pm}(x)\exp[-iE_n^{(\pm)}t]$. The slowly varying amplitude A now is governed by the equation

$$iA_\tau = -(2M)^{-1}A_{\xi\xi} + i\Lambda A + G\chi|A|^2A - i\Upsilon|A|^4A, \tag{31}$$

where $\Upsilon = \int_0^\pi |\varphi^{\pm}|^6 dx$, $g = \varepsilon G$ ($\Upsilon \sim |G| \sim 1$), and other parameters are defined as in (16). We emphasize that, unlike in the cubic case, here we imposed the condition of smallness of the conservative nonlinearity coefficient g, since in this case the effects of the elastic two-body interactions and the inelastic three-body interactions become of the same order and must be accounted for simultaneously.

Now the constant-amplitude solution reads

$$A_{st} = (\Lambda/\Upsilon)^{1/4} e^{-i\Omega\tau}. \tag{32}$$

The number of particles per OL period N and the chemical potential μ depend on the nonlinearity g,

$$N = \sqrt{\frac{\alpha''\gamma + \Delta}{\Upsilon}}, \quad \mu = E_n^{(\pm)} + g\chi\sqrt{\frac{\alpha''\gamma + \Delta}{\Upsilon}}. \tag{33}$$

As can be seen from Eqs. (33), in the case of dissipative quintic nonlinearity, the analytically estimated density of particles in a stationary mode does not depend upon the cubic nonlinearity g [unlike how this happens in the cubic case; see (21)]. The two-body interactions, however, determine the chemical potential μ for given N. In particular, since $\chi > 0$ [see the definition (18)], we have that $\mu < E_n^{(\pm)}$ ($\mu > E_n^{(\pm)}$) when $g < 0$ ($g > 0$). Figure 3 illustrates that the simple analytical estimate for $N(\mu)$ [shown in panels (a) and (c) by dashed lines] is in agreement with the numerical values only in the vicinity of the band edges (this was not true in the case of the cubic dissipative nonlinearity where the domain of quantitative coincidence of the analytical and numerical results was significantly larger; see Fig. 1). The analytical estimates for $g(\mu)$ is in much better agreement with the dependence found numerically [Figs. 3(b) and 3(d)].

Turning to the simple stability analysis of the dissipative Bloch waves, first we notice that the analysis performed in

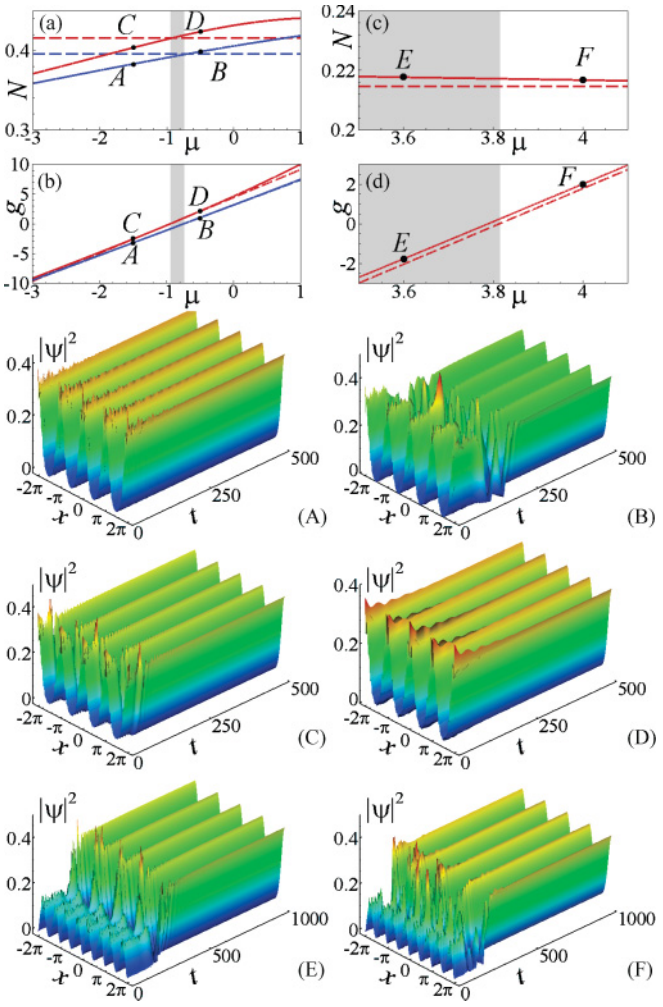

FIG. 3. (Color online) Number of particles N [panels (a), (c)] and cubic nonlinearity g [panels (b), (d)] vs chemical potential μ for $\alpha' = 3.0$, $\alpha' = 0.1$, and $\Delta = 0.0$ calculated analytically (dashed lines) from Eqs. (33) or numerically (solid lines). Gray strips represent the first [in panels (a), (b)] and the second [in panels (c), (d)] bands. In panels (A)–(F) we show temporal evolution of periodic solutions at respective points of panels (a)–(d).

Sec. II C continues to be valid. Moreover, analyzing the stationary solutions (32), we arrive at the conditions (23) obtained earlier for the cubic case. Also similar to the cubic case, direct numerical simulations confirm the validity of (23) for the first band [see Figs. 3(a) and 3(b), where modes A and D are stable while modes B and C are unstable] and their failure for the top of the second band [see Figs. 3(c) and 3(d) showing that modes E and F are unstable].

V. ASSOCIATED DISSIPATIVE LATTICES

As the last point, we observe that the limit of a relatively large potential depth can be described by the tight-binding approximation which is obtained by discretizing Eq. (3) using the expansion

$$\psi(x,t) = \sum_{nk} c_{nk}(t) w_{nk}(x) \tag{34}$$

over the basis of the Wannier functions:

$$w_{nm}(x) = \frac{1}{\sqrt{2}} \int_{-\infty}^{\infty} \varphi_{nq}(x) e^{-i\pi mq} dq. \tag{35}$$

For more precise conditions of the validity of the approximation, as well as for the details of the expansion, we refer to [15], only mentioning here that sufficiently fast convergence of the coefficients ω_{nm} of the Fourier expansion of the energy

$$\omega_{n0} \gg \omega_{n1} \gg \cdots, \quad \omega_{nm} = \frac{1}{2} \int_{-1}^{1} E_n(q) e^{-i\pi mq} dq \tag{36}$$

must be required, allowing one to restrict the consideration to the hopping of only the nearest neighbors.

At this point, however, we emphasize one important feature which distinguishes the Wannier function mapping of the continuous model to a discrete one in the dissipative case. While, in general, the tight-binding limit does not account for a number if important features of the dynamics of the underlying continuum model [15], the tight-binding approximation can be formally performed for a number of the lowest bands (provided the depth of the potential is high enough), still giving reasonable approximation for the static solutions. In the dissipative case the situation is dramatically changed because of the stability properties. Namely, now the tight-binding approximation makes sense only for a band where the periodic solutions are attractors. Even when other bands result in discrete dissipative models with stable solutions, the difference between such solutions and those of the original continuum model grows exponentially already at early stages of the evolution. Therefore, in what follows, we assume that the expansion (34) is performed for the band associated to the stable solutions. Moreover, in accordance with the examples considered earlier in this paper, we choose the first lowest band with $n = 1$. This assumption allows us to drop the band index n in what follows.

Then, using the orthogonality of the Wannier functions, we readily obtain the dissipative discrete NLS equation for the expansion coefficients c_n:

$$i\frac{dc_m}{dt} = \left(1 - i\frac{\alpha''}{\alpha'}\right)(\omega_0 c_m + \omega_1 c_{m+1} + \omega_1 c_{m-1}) + e^{-i\phi} W |c_m|^2 c_m. \tag{37}$$

Here $W = \int_{-\infty}^{\infty} w_{1,m}^4(x)dx$ and we have neglected hopping integrals with the upper bands and among the next-nearest neighbors. The obtained Eq. (37) was considered earlier in [16] (it is also relevant to mention studies of a more general discrete dissipative model in [17]). Therefore, we do not proceed with the further analysis of (37), referring for the study of their modulational instability to the mentioned work.

We complete this last section with the indication that the qubic-quintic dissipative model (29) can be discretized in the similar manner:

$$i\frac{dc_m}{dt} = \left(1 - i\frac{\alpha''}{\alpha'}\right)(\omega_0 c_m + \omega_1 c_{m+1} + \omega_1 c_{m-1}) + gW|c_m|^2 c_m - iB|c_m|^4 c_m, \tag{38}$$

where $B = \int_{-\infty}^{\infty} w_{1,m}^6(x)dx$. This model was also addressed in [16].

VI. CONCLUSIONS

To conclude, we have reported the emergence of nonlinear periodic structures in a NLS equation with a dissipative periodic potential, nonlinear losses, and linear pump. The models describe a BEC loaded in an OL, where the potential created by the light interaction with the condensate accounts for nonelastic interactions of photons with atoms. We addressed nonlinear losses due to two- and three-body interactions. These simple 1D model reveals the existence of stable nonlinear Bloch waves (attractors) to which a large range of the initial data converges. The obtained solutions do not have the linear limit (i.e., the limit of the zero density) and the number of particles is limited from below. In all the simulations performed the observed stable periodic patterns correspond to the lowest band. The existence of the attractor has an important physical consequence: In the described models, loading particles (using the linear pump) is only possible to the given state, which is imposed by the nonlinear losses. By changing the interatomic interactions, one can follow different branches of the stable solutions.

In the meantime the simplest stability analysis performed in the present article does not yet describe all the features of the system which are related, in particular, to the scales comparable with the lattice constant, and thus not accounted for by the multiple-scale expansion. These issues of the theory are left for further studies.

ACKNOWLEDGMENTS

Authors are grateful to F. Kh. Abdullaev for useful comments. Y.V.B. acknowledges partial support from FCT, Grant No. SFRH/PD/20292/2004. The research of V.V.K. was partially supported by the Marie Curie program within the 7th European Community Framework Programme under Grant No. PIIF-GA-2009-236099 (NOMATOS).

[1] *Dissipative Solitons*, edited by N. Akhmediev and A. Ankiewicz, Lecture Notes in Physics, Vol. 661 (Springer, Berlin, 2005); *Dissipative Solitons: From Optics to Biology and Medicine*, edited by N. Akhmediev and A. Ankiewicz, Lecture Notes in Physics, Vol. 751 (Springer, Berlin, 2008).

[2] K. Staliunas and V. J. Sanchez-Morcillo, *Transverse Patterns in Nonlinear Optical Resonators* (Springer-Verlag, Berlin, Heidelberg, 2003); Special issue on *Dissipative Localized Structures in Extended Systems*, edited by M. Tlidi, M. Taki, and Th. Kolokolnikov, Chaos **17**(3) (2007).

[3] I. S. Aranson and L. Kramer, Rev. Mod. Phys. **74**, 99 (2002).

[4] C. J. Pethick and H. Smith, *Bose-Einstein Condensation in Dilute Gases* (Cambridge University Press, Cambridge, UK, 2001).

[5] Y. Kagan, A. E. Muryshev, and G. V. Shlyapnikov, Phys. Rev. Lett. **81**, 933 (1998).

[6] P. O. Fedichev, Yu. Kagan, G. V. Shlyapnikov, and J. T. M. Walraven, Phys. Rev. Lett. **77**, 2913 (1996).

[7] E. A. Burt, R. W. Ghrist, C. J. Myatt, M. J. Holland, E. A. Cornell, and C. E. Wieman, Phys. Rev. Lett. **79**, 337 (1997); T. Kinoshita, T. Wenger, and D. S. Weiss, *ibid.* **95**, 190406 (2005); N. Syassen, D. M. Bauer, M. Lettner, T. Volz, D. Dietze, J. J. García-Ripoll, J. I. Cirac, G. Rempe, and S. Dürr, Science **320**, 1329 (2008).

[8] F. Kh. Abdullaev, A. Gammal, H. L. F. da Luz, and L. Tomio, Phys. Rev. A **76**, 043611 (2007).

[9] T. Gericke, C. Utfeld, N. Hommerstad, and H. Ott, Laser Phys. Lett. **3**, 415 (2006); T. Gericke, P. Würtz, D. Reitz, T. Langen, and H. Ott, Nat. Phys. **4**, 949 (2008).

[10] V. A. Brazhnyi, V. V. Konotop, V. M. Pérez-García, and H. Ott, Phys. Rev. Lett. **102**, 144101 (2009).

[11] H. Sakaguchi and B. A. Malomed, Phys. Rev. E **77**, 056606 (2008); **80**, 026606 (2009).

[12] V. A. Brazhnyi, V. V. Konotop, and M. Taki, Opt. Lett. **34**, 3388 (2009); Phys. Rev. A **80**, 043814 (2009).

[13] B. Kneer, T. Wong, K. Vogel, W. P. Schleich, and D. F. Walls, Phys. Rev. A **58**, 4841 (1998); P. D. Drummond and K. V. Kheruntsyan, *ibid.* **63**, 013605 (2000); C. Yuce and A. Kilic, *ibid.* **74**, 033609 (2006).

[14] V. V. Konotop and M. Salerno, Phys. Rev. A **65**, 021602(R) (2002).

[15] G. L. Alfimov, P. G. Kevrekidis, V. V. Konotop, and M. Salerno, Phys. Rev. E **66**, 046608 (2002).

[16] N. K. Efremidis and D. N. Christodoulides, Phys. Rev. E **67**, 026606 (2003); in *Dissipative Solitons*, edited by N. Akhmediev and A. Ankiewicz (Springer-Verlag, Berlin, Heidelberg, 2005), p. 309.

[17] F. Kh. Abdullaev, A. A. Abdumalikov, and B. A. Umarov, Phys. Lett. **A305**, 371 (2002); F. Kh. Abdullaev, in *Dissipative Solitons*, edited by N. Akhmediev and A. Ankiewicz (Springer-Verlag, Berlin, Heidelberg, 2005), p. 328.